Quasi-Static Finite-Element Analysis of a Skewed Microstrip Crossover

Krzysztof Nyka and Michał Mrozowski, *Member, IEEE*

***Abstract*—In this letter, we present a quasistatic analysis of a microstrip crossover on dielectric substrate. The microstrips are located at different planes and may cross at an arbitrary angle. Capacitances and inductances are calculated from scalar potentials. For magnetostatic formulation, the boundary conditions for scalar potential is introduced by means of partitioning surfaces. The use of adaptive finite element method provides required flexibility with respect to analyzed geometry, optimal discretization and good efficiency.**

***Index Terms*—Adaptive finite-element, discontinuities, inductance, quasistatic, scalar magnetic potential.**

I. Introduction

MICROSTRIPS crossing at right angle have been investigated using a static electric field analysis in [1] and full-wave analysis in [2]. Most recently, a quasistatic electric and magnetic analysis of a right angle microstrip crossover in a multilayer microstrip coupler has been reported in [3]. The capacitances and the inductances of the lumped element representation of discontinuity were derived from a static finite-difference (FD) solution of Laplace equation for electric and magnetic potential. The formulation for the scalar magnetic potential was possible due to the structure's symmetry which allowed the potential to be fixed on symmetry planes serving as magnetic walls. Further simplification resulted form orthogonal orientation of microstrips in the crossover which eliminated the magnetic coupling reflected by zero mutual inductances in the equivalent circuit.

In this letter, we concentrate on the more general case when the microstrips cross at an arbitrary angle (see Fig. 2 for the geometry). The absence of symmetry in a skewed crossover makes it impossible to introduce simple magnetic walls which serve as boundary conditions for magnetic potential. To define the boundary conditions for the scalar magnetic potential, we use the concept of potential partitioning surface [4] introduced in finite-difference magnetostatic analysis. The oblique directions of conductors require more flexible method of discretization than FD. Therefore, we propose a more flexible approach based on the finite element (FE) discretization of Laplace equation. The efficiency and accuracy of our solver is enhanced by adaptive mesh refinement [5] and extrapolation techniques using estimated approximation error [6], [7].

Manuscript received May 9, 2001; revised October 21, 2001. This work was supported by the Foundation for Polish Science under the Senior Scholar Grants Program and the Academic Computing Center TASK in Gdańsk, Poland. The review of this lettter was arranged by Associate Editor Dr. Arvind Sharma.

The authors are with the Department of Electronics, Telecommunications and Informatics, Technical University of Gdańsk, Gdańsk, Poland (e-mail: nyx@pg.gda.pl; mim@pg.gda.pl).

Publisher Item Identifier S 1531-1309(02)00864-4.

II. Magnetic Scalar Potential in Finite-Elements

The existence of magnetic scalar potential ψ in domain Ω such that

$$\vec{H} = -\nabla\psi \tag{1}$$

and satisfying the Laplace equation

$$\nabla\mu\nabla\psi = 0 \tag{2}$$

relies on the following condition

$$\nabla \times \vec{H} = 0 \quad \Leftrightarrow \quad \oint_C \vec{H}\,\vec{dl} = 0 \tag{3}$$

for all closed contours $C \subset \Omega$. This condition may be fulfilled by excluding the currents from Ω and opening all contours that surround the currents. This is realized by cutting the domain with an infinitely thin slit P [Fig. 1(a)] spanning the inner conductors and the ground conductor at the outer boundary. Any closed contour C_I around the current I crosses the boundary of the domain which means that it does not entirely lay inside Ω (i.e., $C_I \not\subset \Omega$) but is geometrically equivalent to a contour $\{P^-, P^+\}$ between the opposite sides of the partitioning slit P. Thus, the integrals along both contours must give the same result

$$I = \oint_{C_I} \vec{H}\,\vec{dl} = \int_{P^-}^{P^+} \vec{H}\,\vec{dl} = \psi(P^+) - \psi(P^-) = \Delta\psi. \tag{4}$$

The partitioning surfaces can be chosen arbitrarily because there is no requirement concerning the absolute values of the potential along P^- and P^+ provided the jump $\Delta\psi$ across the slit is held constant and equal to I.

The partitioning surface should not however disturb the continuity of $\vec{H}$, which together with (1) and (4) yields a pair of boundary conditions on P

$$\psi(P^+) - \psi(P^-) = \Delta\psi = I \tag{5}$$

$$\left.\frac{\partial\psi}{\partial n}\right|_{P^+} + \left.\frac{\partial\psi}{\partial n}\right|_{P^-} = 0. \tag{6}$$

The remaining boundaries are all conducting surfaces Γ_N, on which the magnetic field is governed by the homogenous Neumann condition

$$\left.\frac{\partial\psi}{\partial n}\right|_{\Gamma_N} = 0. \tag{7}$$

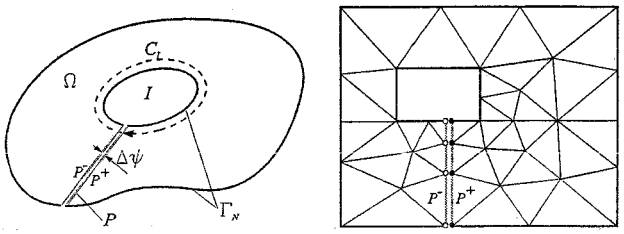

(a) (b)

Fig. 1. Partitioning surface P introducing the magnetic scalar potential jump $\Delta\psi$ equivalent to the current I—(a) the general illustration and (b) the implementation on a finite elements mesh; 2D sections of 3D structures.

It should be noted that the partitioning surface incorporated in the finite element method requires a physical cut into a mesh introducing two boundaries [Fig. 1(b)]. In the finite-difference approach [4], the potential partitioning surface was only a fictitious plane indicating the grid nodes where the differential formulation of derivatives had to be modified according to the boundary conditions.

The condition of the continuity of normal derivatives on P (6) has the same form as the Neumann conditions on Γ_N (7). In the finite-element discretization, they, together, are already built in a weak formulation of the Laplace equation as *natural boundary conditions* and, as such, need not to be applied explicitly.

The condition of constant potential step (5) is implemented as an *essential boundary condition* and its treatment is similar to the periodic conditions with a shift. This yields a symmetric linear equations system $\tilde{A}\psi = \tilde{b}$. More specifically, the condition (5) is used as $\psi_p = \Delta\psi + \psi_q$, where p and q denote the indices of the corresponding nodes at the opposite surfaces of P [black and white dots in Fig. 1(b)]. For adaptive mesh refinement, the above condition is extended to the case when some points do not match exactly nodes at the another side of P and needs interpolation between the vertices of a matching boundary triangle.

III. Analysis of the Crossover

The geometry of the crossover is shown in Fig. 2. The microstrip M_1 lays on the dielectric substrate of relative permittivity ε_r, while the M_2 is buried therein. The microstrips may have a nonzero thickness t. In order to provide the same simulation conditions for a wide range of angles α between the two lines directions, the structure is bounded by a cylindrical closure.

In the static approach, the crossover is considered lumped regardless of its physical size, thus, the equivalent circuit is similar to that of a section of coupled transmission lines (Fig. 2). Capacitances and inductances are derived from separate electro- and magnetostatic analysis, based on two schematics extracted from the overall equivalent circuit (Fig. 3). The elements are computed from the solution of the Laplace equation using the energy formulations

$$W_e = \frac{C}{2V^2} \quad W_m = \frac{L}{2I^2} \tag{8}$$

where $V \equiv \Delta\varphi$ and $I \equiv \Delta\psi$ are excitations given as boundary conditions for electric and magnetic potentials. W_e and W_m are

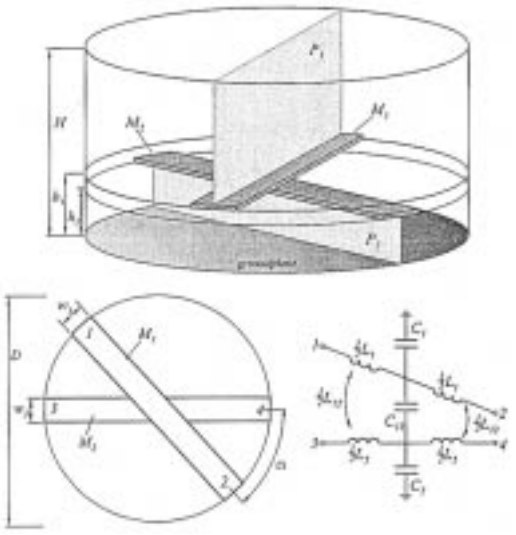

Fig. 2. Geometry of the skewed crossover and its equivalent circuit. P_1 and P_2 are the partitioning surfaces for magnetostatic analysis.

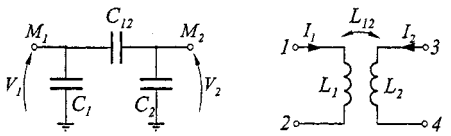

Fig. 3. Equivalent circuits in static electric (capacitances) and magnetic (inductances) analysis.

the total electric and magnetic energy naturally available in the finite elements.

Each circuit element is obtained from the energy for different combination of excitations, as follows:

	V_1	V_2
C_{10}	1	0
C_{01}	0	1
C_{11}	1	1

	I_1	I_2
L_{10}	1	0
L_{01}	0	1
L_{11}	1	1

and

$$\begin{aligned} C_{12} &= \tfrac{1}{2}\left(C_{10} + C_{01} - C_{11}\right) & C_1 &= C_{10} - C_{12} \\ L_{12} &= \tfrac{1}{2}\left(L_{10} + L_{01} - L_{11}\right) & C_2 &= C_{01} - C_{12} \\ & & L_1 &= L_{10} \\ & & L_2 &= L_{01}. \end{aligned} \tag{9}$$

The boundary conditions imposed on a cylindrical housing are different for electric and magnetic simulation. For the former top and bottom covers are conductors of potential $\varphi = 0$, but side surface is the magnetic wall with the Neumann condition in order to isolate the groundplane from the microstrips. In the latter, all surfaces are electric walls with the Neumann condition (7).

IV. Numerical Results

For the sake of comparison, we have analyzed the crossover of physical properties taken from [3], where the orthogonal case has been numerically simulated and experimentally verified in a multilayer directional coupler. The substrate of $\varepsilon_r = 3.25$ has two equal layers $h_2 = h_1 - h_2 = 0.787$ mm. The microstrips M_1 and M_2 have thickness $t = 0.018$ mm and widths $w_1 = 3.1$

TABLE I
NUMERICAL RESULTS FOR DIFFERENT ANGLES α

α	[pF]			[nH]		
	C_1	C_2	C_{12}	L_1	L_2	L_{12}
0°	0.406	1.067	0.983	2.561	2.301	1.213
5°	0.409	1.068	0.974	2.551	2.289	1.209
15°	0.425	1.086	0.918	2.536	2.247	1.125
30°	0.485	1.117	0.765	2.504	2.214	0.901
45°	0.553	1.131	0.616	2.513	2.244	0.645
60°	0.599	1.140	0.520	2.513	2.262	0.402
75°	0.625	1.153	0.473	2.532	2.288	0.186
85°	0.636	1.161	0.459	2.532	2.291	0.049
90°	0.634	1.161	0.459	2.531	2.299	0.0025

TABLE II
COMPARISON OF DEEMBEDDED ELEMENTS FOR $\alpha = 90°$

method	[pF]			[nH]	
	C_1	C_2	C_{12}	L_1	L_2
this analysis	0.0571	0.480	0.464	0.975	1.036
[3]	0.0548	0.472	0.454	0.972	1.03

mm and $w_2 = 2.08$ mm, respectively. The cylindrical housing has diameter $D = 10$ mm and the top cover $H - h_1 = 5h_1 = 7.87$ mm above the substrate.

The equivalent circuit elements of the whole structure computed for different α are listed in Table I. The results for deembedded elements of the right angle crossover ($L_{12} = 0$) are compared with [3] in Table II. The cylindrical housing was replaced by a box of the same height and side walls placed from the microstrips at a distance equal to their widths. The deembedding moved the four ports of the crossover by $w_1 - h_1$ and $w_2 - h_1$ toward the center along M_2 and M_1, respectively.

The size of discretization mesh was between 1053 and 1273 nodes for the initial mesh and between 38 310 and 66 260 nodes for the final mesh (after six steps of adaptive refinement). On the fine mesh, the average approximated discretization error after the correction with an estimated error was 0.3%.

V. CONCLUSION

We have shown that quasistatic analysis of capacitances and inductances in microwave circuits can be efficiently carried out in the framework of finite-elements using scalar potentials for both electric and magnetic field calculations despite the lack of the symmetries allowing the introduction of magnetic walls which enable one to introduce impose boundary conditions on scalar magnetic potential. The adaptive finite-element technique was used to find equivalent circuit of a skewed microstrip crossover. The results for orthogonal case show consistency with previously reported ones.

REFERENCES

[1] S. Papatheodorou, R. F. Harrington, and J. R. Mautz, "The equivalent circuit of a microstrip crossover in a dielectric substrate," *IEEE Trans. Microwave Theory Tech.*, vol. 38, pp. 135–140, Feb. 1990.
[2] S. Papatheodorou, J. R. Mautz, and R. F. Harrington, "Full-wave analysis a microstrip crossover in a dielectric substrate," *IEEE Trans. Microwave Theory Tech.*, vol. 38, pp. 11 439–11 448, Oct. 1990.
[3] D. Jainsson, "Multilayer microstrip directional coupler with discrete coupling," *IEEE Trans. Microwave Theory Tech.*, vol. 48, pp. 1591–1595, Sept. 2000.
[4] S. Lindenmeier and P. Russer, "Design of planar circuit structures with an efficient magnetostatic-field solver," *IEEE Trans. Microwave Theory Tech.*, vol. 45, pp. 2468–2473, Dec. 1997.
[5] F. Bornemann, B. Erdmann, and R. Kornhuber, "Adaptive multilevel—Methods in three space dimensions," *Int. J. Numer. Methods Eng.*, vol. 36, pp. 3187–3203, 1993.
[6] M. Jung and U. Rüde, "Implicit extrapolation methods for multilevel finite element computations," *SIAM J. Sci. Comput.*, vol. 17, no. 1, pp. 156–179, 1996.
[7] K. Nyka, "Multigrid methods in the quick analysis of passive microwave circuits," Ph.D. dissertation (in Polish), Dept. Electron. Inform. Telecommun. Tech. Univ. Gdańsk, Gdańsk, Poland, June 2001.